The He–CaH (2Σ+) interaction. I. Three-dimensional ab initio potential energy surface

Gerrit C. Groenenboom and N. Balakrishnan

Citation: J. Chem. Phys. **118**, 7380 (2003); doi: 10.1063/1.1562946
View online: http://dx.doi.org/10.1063/1.1562946
View Table of Contents: http://jcp.aip.org/resource/1/JCPSA6/v118/i16
Published by the AIP Publishing LLC.

The He–CaH ($^2\Sigma^+$) interaction. I. Three-dimensional *ab initio* potential energy surface

Gerrit C. Groenenboom[a)]
Institute of Theoretical Chemistry, NSRIM, University of Nijmegen, Toernooiveld, 6525 ED Nijmegen, The Netherlands

N. Balakrishnan[b)]
Department of Chemistry, University of Nevada Las Vegas, Las Vegas, Nevada 89154

(Received 28 October 2002; accepted 31 January 2003)

The interaction potential of the He–CaH($^2\Sigma^+$) van der Waals complex is computed with the partially spin-restricted open-shell single and double excitation coupled cluster method with perturbative triples [RCCSD(T)] for more than 3700 geometries. An accurate fit of the three-dimensional potential is made available for the RCCSD as well as the RCCSD(T) results. Also the CaH diatomic potential is calculated at the RCCSD(T) level and shown to be very accurate by comparison of computed vibrational levels and rotational constants to spectroscopic data. In the accompanying paper the potentials are employed in a study of collisions of He with CaH at cold and ultracold temperatures. © *2003 American Institute of Physics.* [DOI: 10.1063/1.1562946]

I. INTRODUCTION

This work is motivated in part by the increasing need for accurate intermolecular potentials to describe collisional and spectroscopic properties of ultracold molecules. Ultracold molecules in selected rovibrational levels have been produced by photoassociation of ultracold atoms,[1–6] electrostatic cooling,[7–13] and the buffer-gas cooling method.[14] Many applications of ultracold molecules have been suggested including high resolution molecular spectroscopy,[15] controlled chemistry,[3,16,17] molecular Bose–Einstein condensates (BECs),[6,18] and quantum computing.[19] Highly accurate molecular potentials have already been derived for a number of alkali metal dimers by combining results of photoassociation experiments and accurate calculations of long-range interatomic potentials. They have become the basis of precise manipulation of atomic BECs through Feshbach spectroscopy. While the photoassociation method has mostly been applied to alkali metal systems the electrostatic and buffer-gas cooling methods are applicable to any molecule with permanent dipole or magnetic moments. This has stimulated a number of theoretical calculations[20–25] which reported rotational, vibrational, and spin-flipping collisions in molecular systems at ultracold temperatures. Because long-range interaction plays an important role in low energy collisions, theoretical studies have mostly focused on van der Waals systems such as He–H_2,[20] He–CO,[21] and He–O_2.[22,25,26] Unfortunately, no experimental data exist for any of these systems at temperatures lower than 1 K though He–CO and He–O_2 are potential candidates for future experiments.

The first molecular system trapped by the buffer gas cooling method is CaH($^2\Sigma^+$). Doyle and co-workers[14] created CaH molecules by laser ablation of CaH_2 and the weak magnetic field seeking states of the molecules were trapped after slowing down by collisions with a buffer gas of ^{3}He. Rate coefficients for elastic, rovibrational inelastic, and spin-flipping transitions in CaH by collisions with ^{3}He were measured at a temperature of about 0.4 K. This is the first such measurement in an atom-molecule system at temperatures lower than 1 K, but no theoretical data are available for comparison with the measurements. Such calculations are extremely important to validate the accuracy of potential energy surfaces needed for ultracold collisional studies. The purpose of this study is to compute the interaction potential for the He–CaH system for the first time, and to provide a suitable analytical representation to use in scattering calculations. In the accompanying paper, we report quantum scattering calculations of rovibrational transitions in CaH induced by collisions with He over a wide range of temperatures and compare the data with the experimental results of Doyle and coworkers.

The potential is computed with the partially spin-restricted open-shell single and double excitation coupled cluster method[27,28] with perturbative triples[28,29] [RCCSD(T)]. Details of the *ab initio* calculations are given in the next section. The analytic fit of the potential is given in Sec. III. We also provide a fit of the interaction potential computed at the RCCSD level. This allows us to investigate the sensitivity of the results of the scattering calculations to the potential by scaling the contribution of the triple excitations. In Sec. IV we present the potentials and discuss their properties and accuracy and Sec. V concludes.

II. *AB INITIO* CALCULATIONS

The calculations are performed with the MOLPRO 2000 package.[30] The molecular orbitals are determined in a restricted open shell Hartree–Fock (ROHF) calculation. In the subsequent RCCSD(T) calculations the Ca ($1s$,$2s$,$2p$,$3s$) or-

[a)]Electronic mail: gerritg@theochem.kun.nl
[b)]Electronic mail: naduvala@unlv.edu

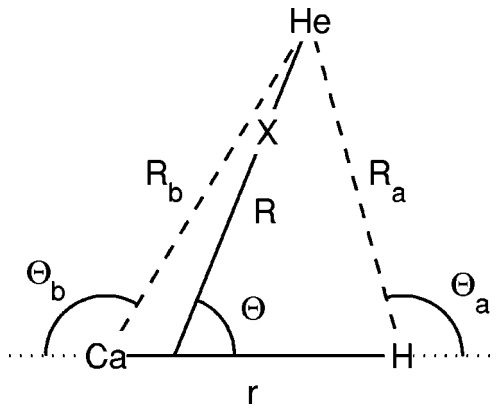

FIG. 1. The coordinates for He–CaH. The "X" indicates the position of the bond functions.

bitals were kept doubly occupied. The interaction energies are determined in a supermolecule approach as $E_{\mathrm{He-CaH}} - E_{\mathrm{He}} - E_{\mathrm{CaH}}$, where the fragments are computed in the same one-electron basis as the complex to avoid introducing a basis set superposition error (BSSE).[31] We use the doubly augmented correlation consistent polarized valence triple zeta (d-aug-cc-pVTZ) basis set[32,33] for the H and He atoms. For the Ca atom we take the 6-311G++$(3df)$ basis set,[34] which we extend by splitting the f polarization function with an exponent-ratio of 2.5 [i.e., using exponents $(\alpha_f/\sqrt{2.5}, \sqrt{2.5}\alpha_f)$] and by adding a g function with $\alpha_g = 1.5$. Added to this is an even tempered set of $(3s3p2d1f1g)$ bond functions on the line connecting the atom and the center of mass of the molecule at a distance of $R/3$ from the atom (where R is the distance between the atom and the center of mass of the molecule, see Fig. 1). We set the exponent-ratio to 3 for the s, p, and d bond functions. The center exponent α_b for the s, p, and d functions was taken equal to the exponent of the f and g bond functions. We optimized α_b in a separate calculation for the Ca–He interaction by maximizing the BSSE corrected interaction energy. This procedure is based on the assumption that the interaction is dominated by dispersion, the description of which is improved by the bond functions. The optimal exponent could be approximated as $\alpha_b = 0.3(9/R_b)^2$, where R_b is the Ca–He internuclear separation. In the calculation of the He–CaH complex we used this expression with R_b replaced by R.

III. THE GRID AND THE POTENTIAL FIT

The full potential was written as the sum of the CaH diatomic potential and the He–CaH interaction energy which we discuss separately.

A. The interaction energy

The interaction energy was calculated for 3732 geometries. To cover the short and intermediate range ($3.5 \leqslant R \leqslant 14$) (all distances in a_0) we employ an equally spaced grid with $\Delta_R = 0.25$ and in the long range ($14 < R \leqslant 20$) we use a logarithmically spaced grid with 7 points. The CaH vibrational coordinate (r) is varied between 3 and 5 with $\Delta_r = 0.25$ for $R \leqslant 14$ and $\Delta_r = 0.4$ for $R > 14$. For the Jacobi angle θ we employ an equally spaced grid with 15 points for $R \leqslant 14$, down to 8 points for $R = 20$. Finally we added 300 points with random geometries for $3 < R < 20$, which were used to test the accuracy of the fit. The results for 40 geometries, almost exclusively in the short range ($R \leqslant 5$), were discarded because of convergence problems in the RCCSD(T) calculation. Also all 116 points where the repulsive interaction is larger than 0.05 E_h were discarded.

The interaction potential is expanded as

$$V(R,\theta,r) = \sum_{i=a,b} V_{\mathrm{sr}}(R_i,\theta_i,r) + V_{\mathrm{lr}}(R,\theta,r). \tag{1}$$

The coordinates R_i and θ_i are defined in Fig. 1. The short range part of the potential is expanded as

$$V_{\mathrm{sr}}(R_i,\theta_i,r) = \sum_{l=0}^{2} e^{-\beta R_i} P_l(\cos\theta_i) s_l^{(i)} + \sum_{n=0}^{3}\sum_{k=0}^{3}\sum_{l=0}^{3} R_i^n e^{-\beta R_i} P_l(\cos\theta_i) r^k \times e^{-\alpha_i r^3} s_{nlk}^{(i)}. \tag{2}$$

For the long range part we take

$$V_{\mathrm{lr}}(R,\theta,r) = \sum_{n=6}^{13}\sum_{l=0}^{n-4} \frac{f_n(\beta R)}{R^n} P_l(\cos\theta) c_{nl}(r), \tag{3}$$

where only terms with $l+n$ is even must be included and

$$c_{nl}(r) = \sum_{k=0}^{1} r^k e^{-\alpha r^3} c_{nlk}. \tag{4}$$

The functions f_n are Tang–Toennies damping functions[35] defined by

$$f_n(x) = 1 - e^{-x}\sum_{k=0}^{n} \frac{x^k}{k!}. \tag{5}$$

The fit procedure was similar to the two-step procedure described in Ref. 36. First we fitted the *ab initio* points for $R > 18$ with only the undamped $n = 6$, 7, and 8 terms of V_{lr} in a weighted linear least squares (WLLS) fit with a weight function $w(R) = R^6$. The coefficients $\{c_{nlk}, n \leqslant 8\}$ determined in this way, as well as the nonlinear parameter α that was used, were kept fixed in the second step of the fitting procedure. All other linear parameters were determined in a WLLS fit with the weight function as given in Eqs. (6)–(9) of Ref. 36 (with $V_0 = 150$ μE_h and $C_6 = 30$). Next, the damping parameter β and all other nonlinear parameters were determined by extensive experimentation following the strategy outlined in Ref. 36.

The largest absolute error in the fit for all points in the attractive region of the potential is about 0.5 μE_h (0.11 cm^{-1}). The largest relative error for all points with either $R > 14$ (i.e., in the long range) or with $V > 5$ mE_h (i.e., in the repulsive part) is 2.5%. These maximum relative and absolute errors hold for the 3289 points that were used in the fit, as well as for the 287 points with random geometries.

After fitting the RCCSD(T) interaction potential we also made a fit of the RCCSD interaction energies. For this fit the

same procedure was used, except that the nonlinear parameters were not reoptimized. The quality of this fit is just as good as for the RCCSD(T) surface.

B. The CaH diatomic potential

Around the interatomic distance of $r=6.1$ a_0 the character of the ground state electronic wave function of CaH changes from essentially ionic (Ca^+H^-) for small r to covalent for large r. In this transition region, the RHF wave function may converge to either state, depending on the initial guess for the orbitals. Still, the RCCSD(T) curves turn out to connect with only a small discontinuity in the first derivative. In order to obtain a smooth ground state potential $[V_{\mathrm{CaH}}(r)]$ we made separate fits of the ''ionic curve'' (computed on a grid with $1.2 \leqslant r \leqslant 6.0$) and the ''covalent curve'' ($6.2 \leqslant r < 30$), switching from one to the other with a polynomial of degree 9. This polynomial is completely fixed by the requirement that at $r=5.89$ and at $r=6.29$ the potential be continuous through the fourth derivative. For the ionic curve energies were computed on a grid with a spacing of 0.1 for $r \leqslant 4$ and 0.2 for $4<r<6$. This part of the potential is represented as

$$V_{\mathrm{CaH}}^{\mathrm{ion}}(r)=\sum_{i=0}^{9} d_i T_i\left(\frac{(r-1.2)-(6-r)}{6-1.2}\right) e^{-\gamma r}, \tag{6}$$

where T_i is a Chebyshev polynomial.[37] The linear parameters d_i as well as γ were fully optimized in a weighted LS fit. We used the weighting function defined in Eq. (8) of Ref. 36, with $V_0=0.1$ E_h. For the covalent part we choose a logarithmically spaced grid of 21 points. In this region we made a fit of the interaction energies of the form

$$V_{\mathrm{CaH}}^{\mathrm{cov}}(r)=\sum_{n=6}^{n_{\max}} c_n r^{-n}, \tag{7}$$

where only the even powers in r are included. Setting $n_{\max}$ to 26 allows a very accurate fit (all points below the dissociation energy agree within 2 cm^{-1} and the largest relative error for $r>6$ is 0.1%), but some precautions are necessary to avoid unphysical behavior beyond the last *ab initio* point at $r=30$. Therefore, we first fit the points with $r>20$ in a three-term expansion with $n_{\max}=10$. This is done in a WLLS fit with the weighting function $w(r)=r^6$. This gives $c_6=-92$. We keep this value fixed and refit all the points with $r>6$ in an expansion with $n_{\max}=26$. For this purpose we use again the WLLS method, but the residual to be minimized is modified by adding the sum of the squares of the contributions of the individual terms in the expansion to the potential in the $r=30$ grid point. This ensures that for $r>30$ the c_6 contribution is dominant and no unphysical oscillations occur. Although our value of c_6 may be a reasonable estimate of the dispersion coefficient for Ca+H, the higher terms in our expansion should not be interpreted in the context of long range theory.

IV. RESULTS AND DISCUSSION

Figure 2 shows cuts of the three-dimensional RCCSD(T) interaction potential with the CaH distance fixed at, $r=3$ a_0, $r=r_e$, and $r=5$ a_0, where we take the experimental equilibrium CaH distance of $r_e=3.7842$ a_0.[38] The minimum of the interaction potential for $r=r_e$ occurs at a skewed geometry with the He atom near the H side of CaH. In the linear geometry there is a saddle point for $\theta=180°$ (He–CaH) and a local minimum for $\theta=0°$ (CaH–He). Around the local minimum the potential for $0 \leqslant \theta \leqslant 22°$ is almost perfectly flat [see panel (b) in Fig. 2], with the energy of the ''transition state'' at $R=10.57$ a_0, $\theta=22°$ only 0.23 μE_h above the energy of the linear geometry. The energy difference is so

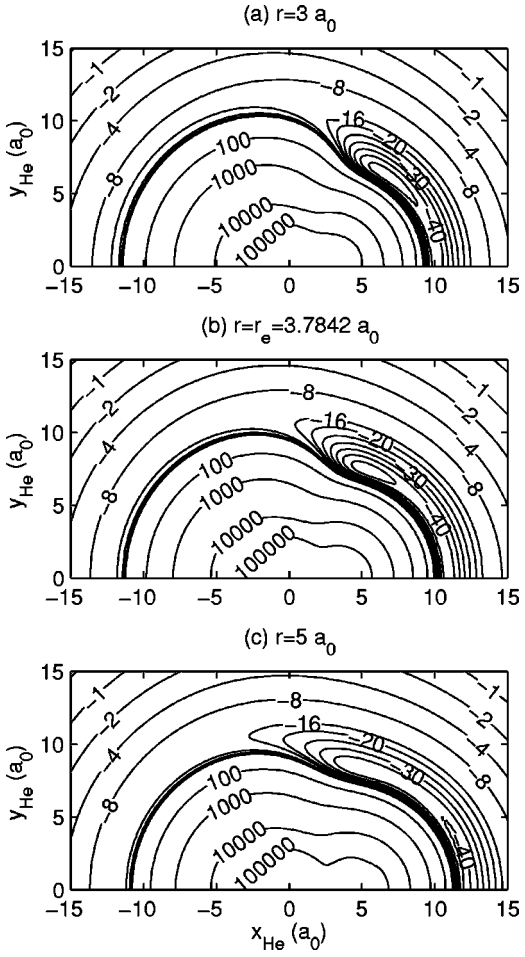

FIG. 2. Cut through the RCCSD(T) interaction potential for three values of the CaH distance (r). The energies of the contour levels are given in μE_h. The origin corresponds to the center of mass of CaH and the position of the He atom is given by $(x_{\mathrm{He}}, y_{\mathrm{He}})=(R\cos\theta, R\sin\theta)$.

TABLE I. This table lists the geometry (R,θ) and the RCCSD(T) interaction potential of the global minimum, the local minimum at $\theta=0°$ (CaH–He) and the saddle point at $\theta=180°$ (He–CaH). The RCCSD values are given in parentheses. The CaH distance is fixed at $r_e=3.7842$ a_0.

	R (a_0)	$\theta(°)$	$V(\mu E_h)$
Minimum	9.15	54.1	−48.31
	(9.27)	(54.7)	(−40.22)
CaH–He	10.89	0.0	−43.05
	(11.04)	(0.0)	(−35.88)
He–CaH	12.50	180.0	−10.06
	(12.74)	(180.0)	(−8.25)

TABLE II. Dependence of the long range coefficients $c_{nl}(r)$ for the He +CaH interaction, computed at the RCCSD(T) level, on the vibrational coordinate. In parentheses the RCCSD values are given.

n,l	$r=3\ a_0$	$r=r_e$	$r=5\ a_0$
6,0	29.6	30.1	34.0
	(27.8)	(28.4)	(31.5)
6,2	−3.13	−1.91	−2.93
	(−2.76)	(−2.41)	(−2.47)
7,1	−158.9	−41.6	258.6
	(−149.3)	(−41.8)	(236.0)
7,3	63.2	107.0	261.0
	(58.1)	(99.3)	(250.1)

small that for a slightly different fit the linear geometry with $\theta=0$ could be a saddle point, rather than a local minimum.

In Table I we report numerical values for the global minimum, the local minimum, and the saddle point (all with $r=r_e$). In this table the interaction energies for the RCCSD surface are given in parentheses. We note that for all geometries the effect of the triple excitations is to increase the strength of the attractive interaction. We also find that the repulsive part of the RCCSD(T) potential is generally less repulsive than the RCCSD potential. The differences are of the order of a few percent. The full set of *ab initio* points is available as an EPAPS document.[39]

In Table II we list the long range coefficients $[c_{nl}(r),n=6,7]$ obtained from our fit for three values of r. In parentheses we give the results for the RCCSD calculation. Note that all of the long range coefficients are somewhat larger at the RCCSD(T) level of theory.

To assess the accuracy of the interaction potential we performed some additional calculations. The long range behavior of the potential is governed by dispersion and induction interactions. As a first test we compute the static polarizability (α) of He in a finite field CCSD calculation (with fields of 0 and 5×10^{-4} a.u.) in a series of four one-electron basis sets[32,33] (aug-cc-pVTZ, d-aug-cc-pVTZ, aug-cc-VQZ, and d-aug-cc-pVQZ). The results, listed in Table III, may be compared to the most accurate literature values of $\alpha=1.383\,169$ (Ref. 40) and 1.383 192.[41] In the d-aug-cc-pVTZ basis used in the calculation of the interaction potential α is 0.38% too high. For the dipole moment of CaH, to our knowledge, no experimental value is available. A value of $\mu=1.0168$ a.u. (Ca^+H^-) was reported[42] for a ROHF +MP2 calculation employing a rather small one-electron basis [(9*s*,7*p*,2*d*) for Ca and (3*s*,2*p*) for H]. With the basis

TABLE III. Calculations with the H- and He-atom one-electron bases as given in the first column. The basis for the Ca-atom was kept fixed as described in Sec. II. We show the polarizability α of He, the dipole moment of CaH at r_e, and the RCCSD(T) interaction energy for two geometries, $(R,\theta,r)=(20,56.25°,3.8)$ and $(9,54°,3.75)$.

Basis	α (a.u.)	μ (a.u.)	$V(R=20a_0)$ (μE_h)	$V(R=9a_0)$ (μE_h)
aug-cc-pVTZ	1.3793	0.9211	−0.559 16	−47.280
d-aug-cc-pVTZ	1.3885	0.9123	−0.558 81	−47.787
aug-cc-pVQZ	1.3842	0.9196	−0.554 95	−48.047
d-aug-cc-pVQZ	1.3852	0.9160	−0.561 68	−48.611

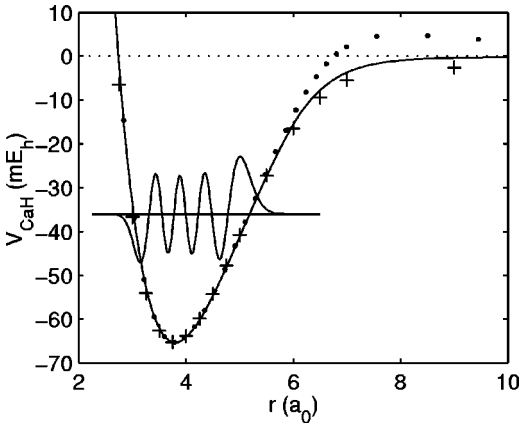

FIG. 3. Our CaH potential (the solid line), together with the semiempirical potential of Ref. 43 (the dots) and the CI potential of Ref. 44 (the plus marks). Also shown in this figure is the $v=7$ vibrational wave function of CaD.

described in Sec. II we find $\mu=0.9123$ a.u. from the first derivative of the energy computed at the RCCSD(T) level in a two-point finite field calculation, with fields of $\pm5\times10^{-5}$ a.u.. Since for Ca no sequence of basis sets similar to the (d-)aug-cc-pVXZ series is available we show in Table III the results of four calculations in which only the basis for the H atom was varied. Since we keep the basis set of Ca fixed the result with the largest H-atom basis is not necessarily the most accurate, but we do expect to get some indication of the accuracy of the result. With the d-aug-cc-pVQZ basis on H, the dipole is 0.4% larger than for the d-aug-cc-pVTZ basis. In Table III we also show the effect of increasing the H- and He-atom bases on the interaction energy in the long range (at $R=20\ a_0$) and near the global minimum. In the largest basis the potential becomes more attractive than in the d-aug-pVTZ basis by 0.5% in the long range and by 1.7% around the minimum. From all these data we conclude that the uncertainty in the interaction energy is of the order of a few percent.

Our calculated CaH diatomic potential is shown as the solid line in Fig. 3. The dots correspond to the semiempirical potential of Martin *et al.*[43] and the plus marks correspond to the configuration interaction (CI) calculation of Leininger *et al.*[44] We computed the vibrational wave functions for CaH and CaD using the sinc-function discrete variable representation (sinc-DVR) method.[45,46] The $v=7$ vibrational wave function for CaD plotted in Fig. 3 corresponds to the highest observed CaD vibrational level[43] (for CaH the highest observed vibrational level[43] is $v=3$). The wave function extends to about $r=6\ a_0$ where all three potentials are in good agreement with each other. However, for $r>6\ a_0$

TABLE IV. Spectroscopic constants of CaH.

r_e (a_0)	B (cm^{-1})	ω_e (cm^{-1})	D_e(cm^{-1})	
3.795	4.205	1296	14 321	This work
3.7842	4.228	1298	⩽14 355	Observed (Refs. 38, 43)
3.783	4.227	1304	14 428	Semiempirical (Ref. 43)
3.76		1284	13 705	CI (Ref. 44)

TABLE V. Calculated T_v and B_v values (cm^{-1}) and the difference with the observed values (Ref. 43) in percent for CaD.

v	T_v	Error in T_v (%)	B_v	Error in B_v (%)
0	0.00		2.163	−0.66
1	908.29	−0.22	2.128	−0.62
2	1796.99	−0.22	2.093	−0.62
3	2666.29	−0.21	2.058	−0.58
4	3516.34	−0.20	2.023	−0.55
5	4347.20	−0.18	1.988	−0.47
6	5158.82	−0.15	1.952	−0.45
7	5951.05	−0.11	1.916	−0.35

the semiempirical potential deviates from the present calculation and the CI results. These results suggest that the semiempirical potential is only accurate in the region where experimental data are available, as might be expected. In Table IV we give the spectroscopic constants for our potential, together with the experimental values and the results for the two other potentials. In Table V we compare the computed term values and rotational constants of CaD with all experimentally observed CaD vibrational levels. The error in our computed vibrational term values is about a factor of five smaller than those computed for the CI calculation of Ref. 44. The excellent agreement of our calculations with experiment is obtained without any scaling of the potential.

Fortran 77 routines to generate the RCCSD and the RCCSD(T) interaction potentials, as well as the CaH diatomic potential are included in the EPAPS document.[39]

V. SUMMARY AND CONCLUSION

We presented accurate fits of the three-dimensional interaction potential for He–CaH computed at the RCCSD and RCCSD(T) levels. We find that the effect of the triple excitations is to make the attractive part of the potential more attractive and the repulsive parts less repulsive. We also provide an accurate fit of the CaH diatomic potential computed at the RCCSD(T) level. This diatomic potential is found to be of very high quality by comparing calculated vibrational levels and rotational constants with spectroscopic data. No spectroscopic data are available for the He–CaH complex. Based on a set of test calculations in different one-electron basis sets we estimate the uncertainty in the interaction potential to be of the order of a few percent. In Paper II we employ the potentials to study collisions of He and CaH at cold and ultracold temperatures, for which experimental data are available. In another paper[47] the potentials will be used to compute spin-flipping transitions in CaH induced by collisions with ^{3}He for which some experimental data are available.

ACKNOWLEDGMENTS

The authors thank Ad van der Avoird and Paul E. S. Wormer for carefully reading the manuscript. N.B. acknowledges support from UNLV in the form of start-up research funds and a New Investigator Award (NIA). This work was partially supported by the National Science Foundation through a grant for the Institute for Theoretical Atomic and Molecular Physics at Harvard University and Smithsonian Astrophysical Observatory.

[1] J. T. Bahns, W. C. Stwalley, and P. L. Gould, J. Chem. Phys. **104**, 9689 (1996).
[2] R. Wynar, R. S. Freeland, D. J. Han, C. Ryu, and D. Heinzen, Science **287**, 1016 (2000).
[3] D. J. Heinzen, R. Wynar, P. D. Drummond, and K. V. Kheruntsyan, Phys. Rev. Lett. **84**, 5029 (2000).
[4] A. N. Nikolov, J. R. Ensher, E. E. Eyler, H. Wang, W. C. Stwalley, and P. L. Gould, Phys. Rev. Lett. **84**, 246 (2000).
[5] J. J. Hope and M. K. Olsen, Phys. Rev. Lett. **86**, 3220 (2001).
[6] E. A. Donley, N. R. Claussen, S. T. Thompson, and C. E. Wieman, Nature (London) **417**, 529 (2002).
[7] H. Bethlem, G. Berden, and G. Meijer, Phys. Rev. Lett. **83**, 1558 (1999).
[8] H. L. Bethlem, G. Berden, A. J. A. van Roij, F. M. H. Crompvoets, and G. Meijer, Phys. Rev. Lett. **84**, 5744 (2000).
[9] H. L. Bethlem, G. Berden, F. M. H. Crompvoets, R. T. Jongma, A. J. A. van Roij, and G. Meijer, Nature (London) **406**, 491 (2000).
[10] F. M. H. Crompvoets, H. L. Bethlem, R. T. Jongma, and G. Meijer, Nature (London) **411**, 174 (2001).
[11] S. Y. T. van de Meerakker, R. T. Jongma, H. L. Bethlem, and G. Meijer, Phys. Rev. A **64**, 041401(R) (2001).
[12] H. L. Bethlem, A. J. A. van Roij, R. T. Jongma, and G. Meijer, Phys. Rev. Lett. **88**, 133003 (2002).
[13] H. L. Bethlem, F. M. H. Crompvoets, R. T. Jongma, S. Y. T. van de Meerakker, and G. Meijer, Phys. Rev. A **65**, 053416 (2002).
[14] J. D. Weinstein, R. deCarvalho, T. Guillet, B. Friedrich, and J. M. Doyle, Nature (London) **395**, 148 (1998).
[15] J. Weiner, V. S. Bagnato, S. Zillo, and P. S. Julienne, Rev. Mod. Phys. **71**, 1 (1999).
[16] D. Herschbach, Rev. Mod. Phys. **71**, S411 (1999).
[17] B. G. Levy, Phys. Today **53**, 46 (2000).
[18] S. J. J. M. F. Kokkelmans, H. M. J. Vissers, and B. J. Verhaar, Phys. Rev. A **63**, 031601 (2001).
[19] D. DeMille, Phys. Rev. Lett. **88**, 067901 (2002).
[20] N. Balakrishnan, R. C. Forrey, and A. Dalgarno, Phys. Rev. Lett. **80**, 3224 (1998).
[21] N. Balakrishnan, A. Dalgarno, and R. C. Forrey, J. Chem. Phys. **113**, 621 (2000).
[22] N. Balakrishnan and A. Dalgarno, J. Phys. Chem. A **105**, 2348 (2001).
[23] P. E. Siska, J. Chem. Phys. **115**, 4527 (2001).
[24] A. V. Avdeenkov and J. L. Bohn, Phys. Rev. A **64**, 052703 (2001).
[25] A. Volpi and J. L. Bohn, Phys. Rev. A **65**, 052712 (2002).
[26] J. L. Bohn, Phys. Rev. A **62**, 032701 (2000).
[27] P. J. Knowles, C. Hampel, and H.-J. Werner, J. Chem. Phys. **99**, 5219 (1993).
[28] P. J. Knowles, C. Hampel, and H.-J. Werner, J. Chem. Phys. **112**, 3106 (2000).
[29] J. D. Watts, J. Gauss, and R. J. Bartlett, J. Chem. Phys. **98**, 8718 (1993).
[30] MOLPRO is a package of *ab initio* programs written by H.-J. Werner and P. J. Knowles, with contributions from J. Almlöf, R. D. Amos *et al.*
[31] S. F. Boys and F. Bernardi, Mol. Phys. **19**, 553 (1970).
[32] T. H. Dunning, Jr., Chem. Phys. **90**, 1007 (1989).
[33] D. E. Woon and T. H. Dunning, J. Chem. Phys. **100**, 2975 (1994).
[34] J.-P. Blaudeau, M. P. McGrath, and L. A. Curtiss, J. Chem. Phys. **107**, 5016 (1997).
[35] K. T. Tang and J. P. Toennies, J. Chem. Phys. **80**, 3726 (1984).
[36] G. C. Groenenboom and I. M. Struniewicz, J. Chem. Phys. **113**, 9562 (2000).
[37] M. Abramowitz and I. A. Stegun, *Handbook of Mathematical Functions* (National Bureau of Standards, Washington, D.C., 1964)
[38] K. P. Huber and G. Herzberg, *Molecular Spectra and Molecular Structure. IV. Constants of Diatomic Molecules* (Van Nostrand Reinhold, New York, 1979).
[39] See EPAPS Document No. E-JCPSA6-118-312316 for a Fortran 77 implementation of the fit of the RCCSD and RCCSD(T) He–CaH interaction potential, the RCCSD(T) CaH potential, and the database of *ab initio* points. A direct link to this document may be found in the online article's HTML reference section. The document may also be reached via the EPAPS homepage (http://www.aip.org/pubservs/epaps.html) or from

ftp.aip.org in the directory /epaps/. See the EPAPS homepage for more information.
[40] M. Jaszuński, W. Klopper, and J. Noga, J. Chem. Phys. **113**, 71 (2000).
[41] D. M. Bishop and J. Pipin, J. Chem. Phys. **91**, 3549 (1989).
[42] T. Kobayashi, K. Sasagane, and K. Yamaguchi, Int. J. Quantum Chem. **65**, 665 (1997).
[43] H. Martin, J. Chem. Phys. **88**, 1797 (1988).
[44] T. Leininger and G.-H. Jeung, J. Chem. Phys. **103**, 3942 (1995).
[45] D. T. Colbert and W. H. Miller, J. Chem. Phys. **96**, 1982 (1992).
[46] G. C. Groenenboom and D. T. Colbert, J. Chem. Phys. **99**, 9681 (1993).
[47] R. V. Krems, A. Dalgarno, N. Balakrishnan, and G. C. Groenenboom, Phys. Rev. A (to be published).